Comparative Medicine
Copyright 2011
by the American Association for Laboratory Animal Science

Vol 61, No 6
December 2011
Pages 484–491

Original Research

Phylogenetic Analysis of *Myobia musculi* (Schranck, 1781) by Using the 18S Small Ribosomal Subunit Sequence

Sanford H Feldman* **and Abraham M Ntenda**

We used high-fidelity PCR to amplify 2 overlapping regions of the ribosomal gene complex from the rodent fur mite *Myobia musculi*. The amplicons encompassed a large portion of the mite's ribosomal gene complex spanning 3128 nucleotides containing the entire 18S rRNA, internal transcribed spacer (ITS) 1, 5.8S rRNA, ITS2, and a portion of the 5′-end of the 28S rRNA. *M. musculi*'s 179-nucleotide 5.8S rRNA nucleotide sequence was not conserved, so this region was identified by conservation of rRNA secondary structure. Maximum likelihood and Bayesian inference phylogenetic analyses were performed by using multiple sequence alignment consisting of 1524 nucleotides of *M. musculi* 18S rRNA and homologous sequences from 42 prostigmatid mites and the tick *Dermacentor andersoni*. The phylograms produced by both methods were in agreement regarding terminal, secondary, and some tertiary phylogenetic relationships among mites. Bayesian inference discriminated most infraordinal relationships between Eleutherengona and Parasitengona mites in the suborder Anystina. Basal relationships between suborders Anystina and Eupodina historically determined by comparing differences in anatomic characteristics were less well-supported by our molecular analysis. Our results recapitulated similar 18S rRNA sequence analyses recently reported. Our study supports *M. musculi* as belonging to the suborder Anystina, infraorder Eleutherenona, and superfamily Cheyletoidea.

Abbreviation: ITS, internal transcribed spacer.

Mites and ticks comprise the subclass Acari in the class Arachnida. According to classical taxonomy based on morphologic characteristics, Acari form 7 orders of which 4 orders contain parasitic forms: Metastigmata (ticks) and Mesostigmata, Prostigmata, and Astigmata (mites).[7] The 3 orders of mites include both free-living forms as well as parasites of plants, invertebrates (arthropods and mollusks), and vertebrates. Fur mites of mammals fall into 2 large families: the Listrophoroidea (Astigmata) and Myobiidae (Prostigmata).[9] Mites of the family Myobiidae are ectoparasites of small marsupial and placental mammals (insectivores, bats, and rodents). Mites in the subfamily Myobiinae are obligate parasites of rodents that exhibit a high degree of host specificity.[10] The Myobiinae include 7 genera: Cryptomyobia, Lavoimyobia, Austromyobia, Idiurobia, Proradfordia, Radfordia, and Myobia. Speciation within each of these genera traditionally is based on chaetoxy, the bristle arrangement of paired setae (birefringent hair-like structures) on the dorsal surface of the idiosoma (body).[8] More recently, taxonomic speciation of Myobiinae examined the anatomic configuration of the gnathostoma (mouthparts), specialization of the anterior pair of legs (leg I) used to grasp the pelage of the host, structural shape of the genital shield, and anatomic location and number of paired setae on the genital shield and dorsum of the hysterosoma (abdomen).[4]

Received: 14 Jun 2011. Revision requested: 22 Jul 2011. Accepted: 23 Jul 2011.
Center for Comparative Medicine, University of Virginia, Charlottesville, Virginia.
**Corresponding author. Email: shf2b@virginia.edu*

Myobia musculi (Schranck, 1781; Trombidiformes: Myobiidae) is a skin-dwelling nonburrowing parasitic fur mite that infests house mice (*Mus musculus*), sometimes laboratory mice, and rarely laboratory rats or other rodents.[17] This mite preferentially populates the head and neck of infested mice, is intimately associated with the skin, and presumably feeds on sebaceous secretion from hair follicles and lymph secreted from the inflamed skin.[12] In contrast, *Myocoptes musculinus* (Koch 1840) populates the mouse's head and dorsum. The severity of dermal and systemic pathology in house mice in response to *M. musculi* acariasis is dependent on the strain of mice, duration of infestation, and ability of the mice to remove the mites by grooming.[27] Geographically, *M. musculi* is distributed worldwide[19,26] with a low but persistent prevalence of 0.11% to 0.12%, according to submissions from research colonies to diagnostic laboratories.[24,25] Compared with its incidence on laboratory mice, *M. musculi* likely is more prevalent on wild mice and mice maintained in pet stores.[3]

Recently several laboratories have reexamined mite phylogeny by using DNA sequence comparison as a means of taxonomic classification[6,18] or by combining anatomic characteristics with rRNA sequence analyses for taxonomic analysis.[22] Taxonomic relationships of mites based on 18S rRNA gene sequences generally agree with the morphologic taxonomic classification.[18] During routine mouse barrier health surveillance at our institution, *Myobia musculi* was detected on one sentinel in one of our facilities. We isolated *M. musculi* DNA and use high-fidelity PCR to amplify

and sequence a portion of the ribosomal gene complex so that we might examine its phylogeny by molecular methods. Here we describe a significant portion of the ribosomal gene complex of *M. musculi* and our molecular phylogenetic analyses based upon its 18S rRNA primary sequence.

Materials and Methods

DNA isolation. One Crl:CFW (SW) female sentinel mouse was obtained, housed, and euthanized under our sentinel animal protocol approved by the University of Virginia IACUC. Adult *M. musculi* were collected under a dissection microscope and stored in 100% ethanol at −20 °C until processed for DNA isolation. Approximately 25 adult mites were placed in a sterile 1-mL glass grinder to which 180 µL ATL buffer (DNeasy Spin Column Kit, Qiagen, Valencia, CA). Mites were ground until no longer visible, the solution was transferred to a 1-mL microfuge tube, and 20 µL (20 mg/mL) proteinase K was added. The mixture was mixed briefly on a vortexer and incubated at 55 °C for 1 h with vigorous shaking, followed by processing according to the manufacturer's recommendations for animal tissues. The DNA was eluted from the spin column by using 50 µL high-resistivity water heated to 70 °C followed by centrifugation.

PCR partial amplification of the ribosomal gene complex. The 18S rRNA gene was amplified by using previously described primers[6] (sense primer, 5′ CTT GCT CAA AGA TTA AGC CAT GCA 3′; antisense primer, 5′ TGA TCC TTC CGC AGG TTC ACC T 3′). The ITS and 5.8S regions were amplified by using published primers [20] (sense primer, 5′ AGA GGA AGT AAA AGT CGT AAC AAG 3′; antisense primer, 5′ CCC CCT GAA TTT AAG CAT AT 3′). The 25-µL amplification reactions contained 1.25 U HotStart Ex *Taq* polymerase (Takara Mirus, Otsu Shiga, Japan), 2 mM magnesium, 200 µM each dNTP, and 10 pM each primer. Amplification was performed on a Robocycler 9600 gradient (Stratagene, La Jolla, CA). For the 18S rRNA gene, the thermal cycler settings were: 'hot start' of 10 s at 98 °C; 32 cycles of denaturation at 98 °C for 10 s, annealing at 65 °C for 30 s, and extension at 72 °C for 2.5 min; and a final extension at 72 °C for 5 min. For the ITS, 5.8S rRNA, and partial 28S rRNA regions, reaction conditions remained the same, except that the annealing temperature was set at 55 °C and the polymerase extension time was 1 min. To visualize the resulting amplicons, 2-µL samples of each PCR reaction were separated by horizontal slab gel electrophoresis and stained with 0.5 µg/mL ethidium bromide; molecular size markers (Bioline Hyperladder II, Tauton, MA) were included, and the results were documented (Gel Doc, Biorad, Hercules, CA).

Amplicon cloning and sequence determination. The amplicons were cloned into TOPO pCR4 plasmid (Invitrogen, Carlsbad, CA) and transfected into One-Shot TOP10 *E. coli* cells (Invitrogen). Four clones from each amplicon were purified and digested with *Eco*R1 (New England Biolabs, Ipswich, MA) to verify the presence of the amplicon prior to sequencing. The clones were submitted to Davis Sequencing (Davis, CA) and sequenced in the forward and reverse directions by using the T3 and T7 plasmid initiation sites. Sequences obtained were aligned by using Omiga 1.1 (Accelerys, San Diego, CA), and nucleotide positions of sequence ambiguity resolved by 'majority rule.' Regions of overlap of the amplicons (18S rRNA and ITS1) were identified by alignment of the terminal 100 nucleotides of the 3′ end of the 18S amplicon and 100 nucleotides of the 5′ end of the ITS–28S amplicon.

Phylogenetic analysis of 18S rRNA sequence. The NIH database GenBank was searched by using the keywords 'Prostigmata' and '18S rRNA'; this query returned 448 sequences representing 42 unique species of mites with sufficient 18S rRNA gene deposited for use in our analysis (Figure 1). The 18S rRNA sequence of *Dermacentor andersoni* (accession no., DCN18SR) was included in the analyses to root the resulting phylograms. The sequences were aligned by using Clustal X (Clustal, Dublin, Ireland).[14]

The Clustal X alignment was optimized manually and truncated to identical 3′ and 5′ termini in all sequences. The resulting 18S rRNA sequence of *M. musculi* used for analyses was 1524 nucleotides in length. The Clustal alignment was output in FASTA, PHYLIP interleaved, and NEXUS formats. The FASTA formatted alignment was imported into jModelTest 0.1.1 and the most statistically appropriate nucleotide substitution model identified.[23] Phylogenetic analyses using maximum likelihood were performed by using the PHYLIP suite of software programs.[11] The 100 datasets generated underwent bootstrap analysis by using DNAML with the following parameters: random number seed, 3; jumble, 3; global rearrangement, off. The nucleotide substitution model was determined by jModelTest, and the *D. andersoni* sequence used as the outgroup. The number of trees in agreement at each node was determined by using CONSENSE; nodal values below 50% were considered insufficiently supported and those branches collapsed in the resulting phylogram.

Bayesian inferential analysis used the program Mr Bayes,[1] with parameters set to 4 × 4 noncoding sequence and the substitution model input that was determined by jModelTest. We ran 3 million generations of posterior probability calculations with a sampling frequency of 1000, program default values were used for all other parameters, and branch lengths were not constrained. At the end of the analysis, the standard deviation of split frequencies was less than 0.01, and a 'burn-in' value of 2500 was input.

Phylograms were displayed by using TreeView[21] rooted to *D. andersoni* and exported as Windows Enhanced metafiles. Text editing of phylograms was performed by using Corel Draw (Corel Corporations, Ottawa, Canada).

Identification of the 5.8S rRNA region. To identify the 5.8S rRNA gene region, we used a Clustal X alignment of the 172-nucleotide 5.8S rRNA gene of *Demodex folliculorum* (GenBank accession no., AM904564; nucleotides 317 through 489), with 874 nucleotides comprising the ITS1–5.8S–ITS2 regions of *M. musculi*, and output the results in FASTA format.[14] The alignment was analyzed further by using the RNAalifold webserver (http://rna.tbi.univie.ac.at/cgi-bin/RNAalifold.cgi), which identified the *M. musculi* 5.8S rRNA region by conservation of RNA secondary structure.[2,15,16] The thermodynamic characteristics of the entire ITS1–5.8S–ITS2 secondary folding were determined by using RNAfold software on the Vienna server (http://rna.tbi.univie.ac.at/cgi-bin/RNAfold.cgi).[13] The 179-nucleotide *M. musculi* 5.8S rRNA secondary structure was recalculated by using RNAfold on the Vienna server, and the thermodynamically most favorable structure was determined independent of the ITS regions.

Results

The ribosomal sequence of *Myobia musculi*. The *M. musculi* 18S rRNA PCR amplicon was 1807 nucleotides in length. The ITS and 5.8S PCR amplicon was 1374 nucleotides. The total portion of the *M. musculi* ribosomal gene complex sequenced spanned 3128 nucleotides, with the 2 fragments overlapping by 53 nucleotides.

Organism	Accession no.	Suborder	Infraorder	Superfamily
Agistemus sp. AP-2010	HM070366	Anystina	Eleutherengona	Raphignathoidea
Anystis sp.	AF022026	Anystina	Anystae	Anystoidea
Anystis sp. AP-2010	HM070361	Anystina	Anystae	Anystoidea
Arrenurus sp. AP-2010	HM070349	Anystina	Parasitengona	Arrenuroidea
Balaustium sp. KD-2007	EF203775	Anystina	Parasitengona	Erythraeoidea
Bdellodes sp. AP-2010	HM070358	Eupodina		Bdelloidea
Cheletomimus wellsi	HM070363	Anystina	Eleutherengona	Cheyletoidea
Dactylothrombium pulcherrimum	GQ864281	Anystina	Parasitengona	Trombidioidea
Erythracarus sp. AP-2010	HM070359	Anystina	Anystae	Anystoidea
Eupodidae sp. AMUENV025	GQ864273	Eupodina		Eupodoidea
Halacarus sp. AP-2010	HM070350	Eupodina		Halacaroidea
Horreolanus orphanus	AY620907	Anystina	Parasitengona	Arrenuroidea
Hydrachna sp. AP-2010	HM070348	Anystina	Parasitengona	Hydrachnoidea
Hygrobates longipalpis	GQ864277	Anystina	Parasitengona	Hygrobatoidea
Johnstoniana errans	GQ864282	Anystina	Parasitengona	Trombidioidea
Labidostomma luteum	GQ864278	Eupodina		Labidostommatoidea
Labidostomma sp. RHT-1997	AF022034	Eupodina		Labidostommatoidea
Limnesia sp. AP-2010	HM070346	Anystina	Parasitengona	Hygrobatoidea
Leptus sp. AP-2010	HM070355	Anystina	Parasitengona	Erythraeoidea
Linopodes motatorius	GQ864270	Eupodina		Eupodoidea
Linopodes sp. AMUENV071	GQ864274	Eupodina		Eupodoidea
Microcaeculus sp. JCO-1999	AF287232	Anystina	Anystina incertae sedis	Caeculoidea
Microtrombidium sp. AP-2010	HM070352	Anystina	Parasitengona	Trombidioidea
Neochelacheles messersmithi	AY620908	Anystina	Eleutherengona	Raphignathoidea
Oudemansicheyla sp. AP-2010	HM070362	Anystina	Eleutherengona	Cheyletoidea
Partnunia steinmanni	GQ864276	Anystina	Parasitengona	Hydryphantoidea
Penthaleus cf. major MD-2010	GQ864271	Eupodina		Eupodoidea
Penthaleus minor	AY620909	Eupodina		Eupodoidea
Poecilophysis sp. AP-2010	HM070360	Eupodina		Eupodoidea
Recifella sp. AP-2010	HM070347	Anystina	Parasitengona	Hygrobatoidea
Rhagidia sp. AMUENV016	GQ864272	Eupodina		Eupodoidea
Rhagidia sp. AMUVe007	GQ864275	Eupodina		Eupodoidea
Rhombognathus levigatoides	HM070351	Eupodina		Halacaroidea
Scolotydaeus corticicola	HM070367	Anystina	Anystina incertae sedis	Paratydeoidea
Smaridiidae sp. AP-2010	HM070364	Anystina	Parasitengona	Erythraeoidea
Sonotetranychus sp. AP-2010	HM070371	Anystina	Eleutherengona	Tetranychoidea
Sperchon violaceus	GQ864279	Anystina	Parasitengona	Sperchontoidea
Spinibdella sp. AP-2010	HM070368	Eupodina		Bdelloidea
Syringophilidae sp. AMUTor1	GQ864269	Anystina	Eleutherengona	Cheyletoidea
Tenuipalpus heveae	HM070370	Anystina	Eleutherengona	Tetranychoidea
Trombiculidae cf. Hoffmaniella sp. AP-2010	HM070354	Anystina	Parasitengona	Trombiculoidea
Trombidiinae sp. AMUENV055	GQ864280	Anystina	Parasitengona	Trombiculoidea

Figure 1. Trombidiformes used in the phylogenetic analysis. Taxonomy: Eukaryota; Metazoa; Arthropoda; Chelicerata; Arachnida; Acari; Acariformes; Trombidiformes; Prostigmata.

The 28S rRNA sequence begins at nucleotide 2692, with the ITS1–5.8S–ITS2 region lying between nucleotides 1808 and 2691, according to BLAST alignment of the sequence we determined with mite sequences in GenBank (data not shown). A BLAST alignment of the 874 nucleotides comprising the ITS1–5.8S–ITS2 region demonstrated no significant sequence similarity to any deposits in the NIH GenBank. The nucleotides encoding the 5.8S rRNA region were determined by secondary structural analysis. Table 1 provides details of the nucleotide positions of each of the rRNA regions and their %GC content. The partial sequence of *M. musculi* ribosomal gene complex has been deposited in GenBank under accession no. JF934703.

The 5.8S rRNA region. The free energy determined by thermodynamic ensemble prediction of centroid structure (a mathematical determination of the most energetically favorable secondary structure) for the ITS1–5.8S–ITS2 region is –210.71 kcal/mol. The predicted secondary structure (Figure 2 A) showed a very high degree of internal complimentary base-pairing, particularly in the ITS regions. This substantial amount of internal base-pairing is reflected in the high percentage (91.74%) of A and T residues in this region between the 18S and 28S rRNA genes. The secondary structural alignment of the *M. musculi* ITS1–5.8S–ITS2 with the 5.8S rRNA region of *D. folliculorum* identified the area of conserved 5.8S rRNA structure in the *M. musculi* 5.8S rRNA region (Figure 2 A). Recalculation of the *M. musculi* 5.8S rRNA secondary

Table 1. Characteristics of *Myobia musculi* ribosomal regions

	18S rRNA	ITS1	5.8S rRNA	ITS2	28S rRNA partial
Nucleotide position	1–1807	1808–2412	2413–2591	2592–2684	2685–3128
Size (nucleotides)	1807	605	179	101	436
%GC content	45.10	8.26	24.59	19.35	37.16

structure independent of the ITS regions yielded a conformation similar in shape to that classically shown for this region in other eukaryotic species.[5] The recalculated 5.8S rRNA centroid ensemble free energy is –38.31 kcal/mol, and the secondary structure of the 5.8S rRNA region is depicted in Figure 2 B. A BLAST search of the *M. musculi* 5.8S rRNA 179-nucleotide primary sequence demonstrated no sequence similarities currently deposited in the NIH GenBank database.

Phylogenetic analysis using 18S rRNA sequence. The size of the 18S rRNA sequences of 42 prostigmatid mites in this study ranged from 1494 to 1927 nucleotides. The longest sequences were those belonging to *Tenuipalpus heveae* (1927nt) and *Sonotetranychus* spp. AP-2010 (1845 nucleotides), with the remaining mites having sequences of 1593 nucleotides or less. Four defined regions[5] within the 18s rRNA in *T. heveae* and *Sonotetranychus* spp. AP-2010 account for the gene expansion in these species: insertion at the V2/V4 region, helix E23-2, helix E23-12, and helix 43. The 18S rRNA multiple sequence alignment contained 1971 characters, of which 785 were conserved and 1186 were informative. By using jModeltest 0.1.1, we analyzed the 18S sequence Clustal X alignment to identify the best evolutionary model among 88 potential models for subsequent phylogenetic analyses. Both Akaike information criterion and Bayesian information criterion (measures of the goodness-of-fit of the selected statistical model) identified a generalized time reversal model (6 independent nucleotide substitution rates and 4 equilibrium frequencies, 1 for each nucleotide) with γ distribution of rate variation among sites (a probability model based on 2 parameters: shape and scale). The specific transition (purine to purine or pyrimidine to pyrimidine) and transversion (purine to pyrimidine or pyrimidine to purine) frequencies of the alignment were: AC, 1.3099; AG, 3.2251; AT, 2.4708; CG, 0.7425; CT, 5.2558; and GT, 1. The calculated log likelihood score (a measure of how likely the chosen parameters fit the observed data) was –17218.29 derived from 95 optimized free parameters (unequal base frequencies, variation of base changes, 85 branch lengths, and topology) and a γ shape parameter of 0.2810. The frequency of base occurrences in the alignment were: A, 0.2515; C, 0.2117; G, 0.2621; and T, 0.2747.

The results of maximum likelihood analysis are shown in Figure 3 and Bayesian inference in Figure 4. Bayesian inference clearly shows that the suborder Anystina arose as a divergence from the suborder Eupodina, forming a sister clade to the Halacaroidea (*Rhombognathes levigatoides* and *Halacarus sp. AP-2010*); maximum likelihood analysis did not demonstrate this relationship. Moreover Bayesian inference shows the divergence of the Anystina into the 2 infraorders Eleutherengona and Parasitengona, a finding not determined by maximum likelihood analysis. *Myobia musculi* is within the clade of suborder Anystina, infraorder Eleutherengona, superfamily Cheyletoidea that in our analysis consisted of members *Oudemansicheyla sp. AP-2010*, *Cheletomimus wellsi*, and *Syringophilidae sp. AMUTor1*. *Neochelacheles messersmithi* and *Agistemus sp. AP-2010*, 2 members of the superfamily Raphignathoidea that are typically characterized as being within this infraorder, had infraordinal relationships that were poorly supported by either method in our analysis. Both analyses support the infraorder Eleutherengona as a single clade, with clear divergence of the superfamily Tetranychoidea (*Tenuipalpus heveae* and *Sonotetranychus sp. AP-2010*) from the Cheyletoidea. The infraordinal interspecies phylogenetic relationships within Eleutherengona were portrayed in an identical manner by Bayesian inference and maximum likelihood methods.

Species included within the suborder Parasitengona are supported as a clade by Bayesian inference; however, only some infraordinal relationships were identified by maximum likelihood. Both methods of analyses support some relationships within superfamilies; however, not all relationships described by anatomic characteristics were supported. For example, the order of lineage divergence of Parasitengona supported by both analyses is Hydrachnoidea and Arrenuroidea as sister clades, with Hygrobatoidea diverging from Hydrachnoidea. Bayesian inference shows the genera *Limnesia sp. AP-2010* basal to the superfamily Sperchontoidea with an evolutionary progression from which Hydryphantoidea arose and later the Hydrachnoidea lineage. Thereafter, the sister clades Arrenuroidea and Hygrobatoidea diverged. However, the direct relationship of *Limnesia sp. AP-2010* to the superfamily Hygrobatoidea is poorly supported in both our analyses. The superfamily Trombidioidea lineage was derived from the Trombiculoidea in both analyses. These 2 superfamilies appear as a single sister clade to *Limnesia sp. AP-2010*. However, *Trombiculidae cf. Hoffmaniella sp. AP-2010*, traditionally characterized in the Superfamily Trombiculoidea, appears to be more closely related to Trombidioidea (*Dactylothrombium pulcherrimum* and *Microtrombidium sp. AP-2010*) in both of our analyses. Another discrepancy of our results with historical phylogeny places *Johnstoniana errans*, historically ascribed to the superfamily Trombidioidea, as the most primitive member of the infraorder Parasitengona followed by *Trombidiinae sp. AMUENV055*, which historically is ascribed to the Superfamily Trombiculoidea. The most primitive member of the Anystina lineage in our Bayesian analysis was *Microcaeculus sp. JCO-1999* (superfamily Caculoidea), from which *Erythracarus sp. AP-2010* (Superfamily Anystoidea), superfamily Erythraeoidea (members *Leptus sp. AP-2010* and *Smaridiidae sp. AP-2010*, and later *Blaustium sp. KD-2007*) and all other members of Parasitengona lineage arose consecutively. Both of our analyses show *Anystina* spp., *Anystina sp. AP-2010*, and *Scolotydaeus corticicola* as separately belonging to the suborder Eupodina rather than the suborder Anystina.

Relationships among members of the suborder Eupodina were more tenuous in our analyses, with both analyses supporting a single clade in superfamily Labidostommatoidea (*Labidostomma luteum* and *Labidostomma sp. RHT-1997*) and 2 clades in Superfamily Eupodoidea (*Rhagidia sp. AMUe007*, *Rhagidia sp. AMUENV016*, and *Poecilophysis sp. AP-2010*; and *Bdellodes sp. AP-201*, *Pentathaleus minor*, and *Pentathaleus cf. major MD-2010*). The most

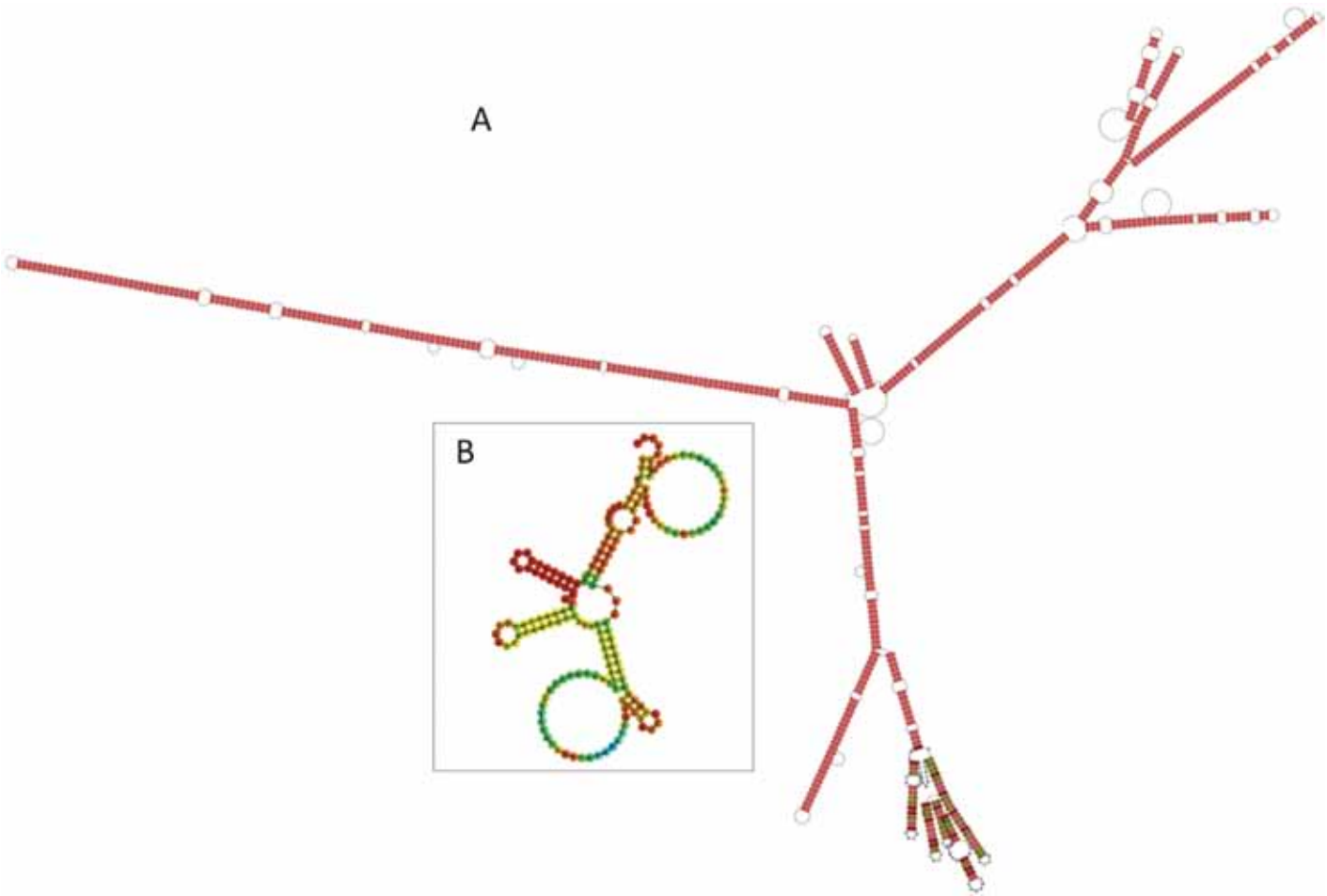

Figure 2. (A) The secondary structure of the *M. musculi* ITS1–5.8S rRNA–ITS2 region as generated by the RNAalifold webserver. The region identified as 5.8S rRNA by structural homology with the *D. folliculorum* 5.8S region is multicolored at the base. (B) The secondary structure for the 5.8S rRNA region of *M. musculi* was recalculated in the absence of the ITS regions by using the Vienna webserver RNAfold software.

primitive superfamily in our Bayesian analysis was Labidostommatoidea, lying at the Metastigmata (tick) root. Bayesian inference places *Spinibdella sp. AP-2010* (superfamily Bdelloidea) as the next most ancestral sequence, from which the Eupodoidea (*Rhagidia sp. AMUe007*, *Rhagidia sp. AMUENV016*, and *Poecilophysis sp. AP-2010*) derived. Subsequently sequences belonging to members of the suborder Anystina (*Microcaeculus sp. JCO-1999* and *Erythracarus sp. AP-2010*) appeared. An additional Eupodoidea lineage containing *Bdellodes sp. AP-201*, *Pentathaleus minor*, and *Pentathaleus cf. major MD-2010* sequences diverged, followed by the lineages containing the superfamily Erythraeoidea and the remaining members of the suborder Anystina. One additional clade of Eupodina (*Eupodidae sp. AMEUNV025*, *Linopodes motatorius*, and *Linopodes sp. AMUENV071*) derived from the superfamily Halacaroidea (*Halacarus sp. AP-2010* and *Rhombognathus levigatoides*), and sandwiched between these 2 clades are 3 members historically described as belonging to the suborder Anystina (*Scolotydaeus corticicola*, *Anystis* spp., and *Anystis sp. AP-2010*). Our maximum likelihood analysis supported the following 2 phylogenetic mixing of species in the suborders Anystina and Parasitengonas: *Rhombognathus levigatoides*, *Anystis* spp., and *Anystis sp. AP-2010*; and *Scolotydaeus corticicola*, *Eupodidae sp. AMEUNV025*, *Linopodes motatorius*, and *Linopodes sp. AMUENV071*.

Discussion

The current investigation was undertaken to obtain fundamental DNA sequence information about *Myobia musculi*, a common ectoparasite of laboratory mice, and to use this sequence to examine the phylogeny of this organism. We seized the opportunity to examine *M. musculi* at the molecular level prior to eradicating the parasite. In doing so, we successfully determined the nucleotide sequence of a large portion of the ribosomal gene complex from *M. musculi*. We discerned various ribosomal gene regions and used a large portion of the 18S rRNA to reexamine the phylogeny of this common fur mite of laboratory mice. Our phylogenetic analysis of *M. musculi* was consistent with previous taxonomic classifications based on morphologic characteristics: *M. musculi* is in the suborder Anystina, infraorder Eleutherenona, and superfamily Cheyletoidea.

We were surprised that the 5.8S rRNA sequence among divergent taxa of mites was not conserved, unlike portions of the 18S rRNA and 28S rRNA sequences. This lack of 5.8S rRNA sequence conservation initially hampered our ability to identify this re-

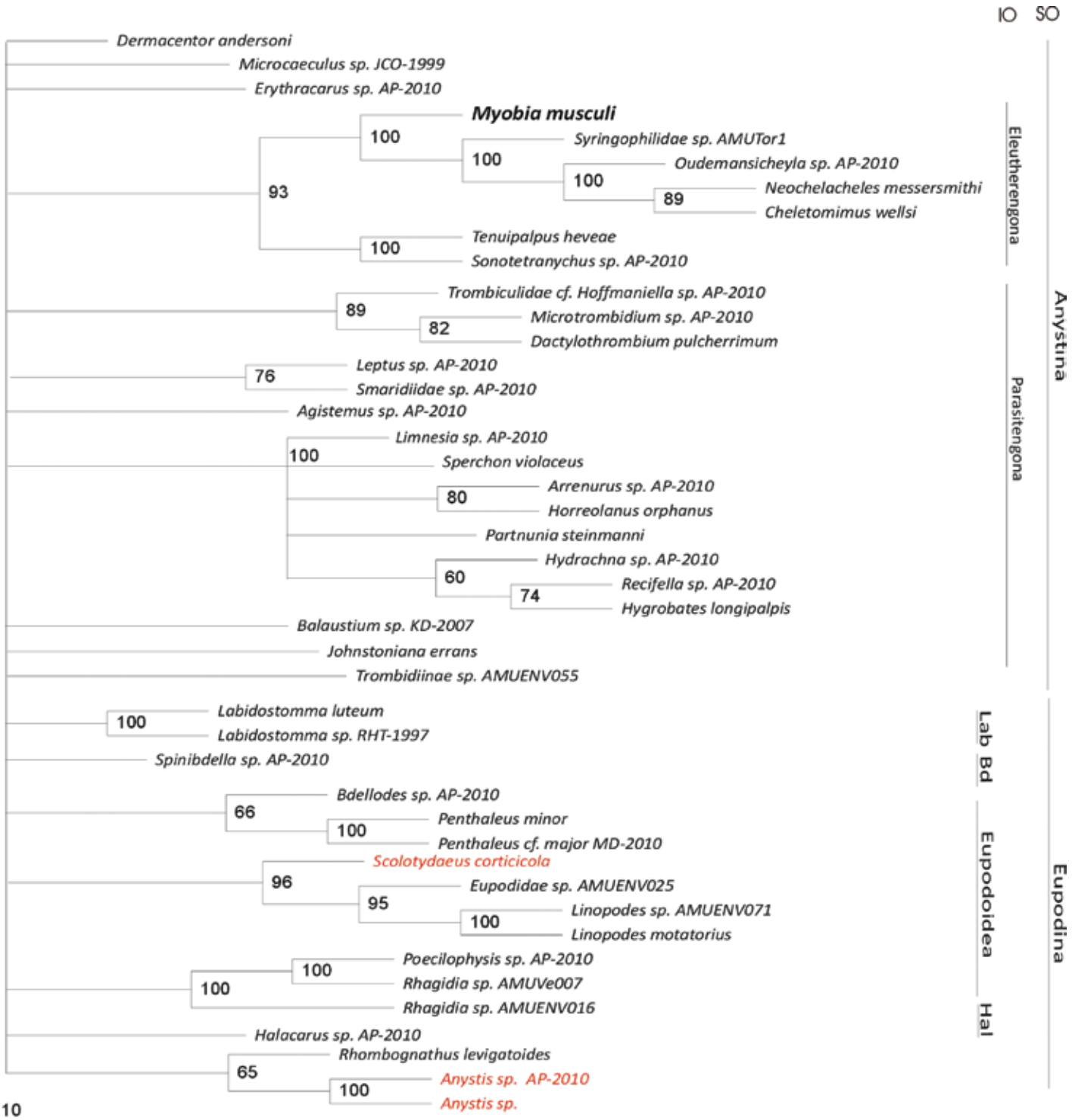

Figure 3. Depicted is the phylogram generated by PHYLIP DNAML maximum likelihood analysis of the *M. musculi* 18S rRNA sequence alignment showing the relationships among the Trombidiformes analyzed. Hal, Halacaroidea; Bd, Bdelloidea; Lab, Labidostommatoidea. Species highlighted in red are discrepant between historical and molecular taxonomic classification. The size bar represents the horizontal branch length associated with 10 nucleotide substitutions.

gion in the ITS1–5.8S rRNA–ITS2–28S rRNA partial amplicon. The sequence of investigation that ensued required that we first perform our phylogenetic investigation to identify a Cheyletoidea mite whose 5.8S rRNA sequence had been deposited in GenBank. A search of the GenBank nucleotide database using the terms 'Cheyletoidea' and '5.8S rRNA' returned a single accession (AM904564), which was for *Demodex folliculorum*. We extracted the 5.8S rRNA sequence from this accession and hypothesized

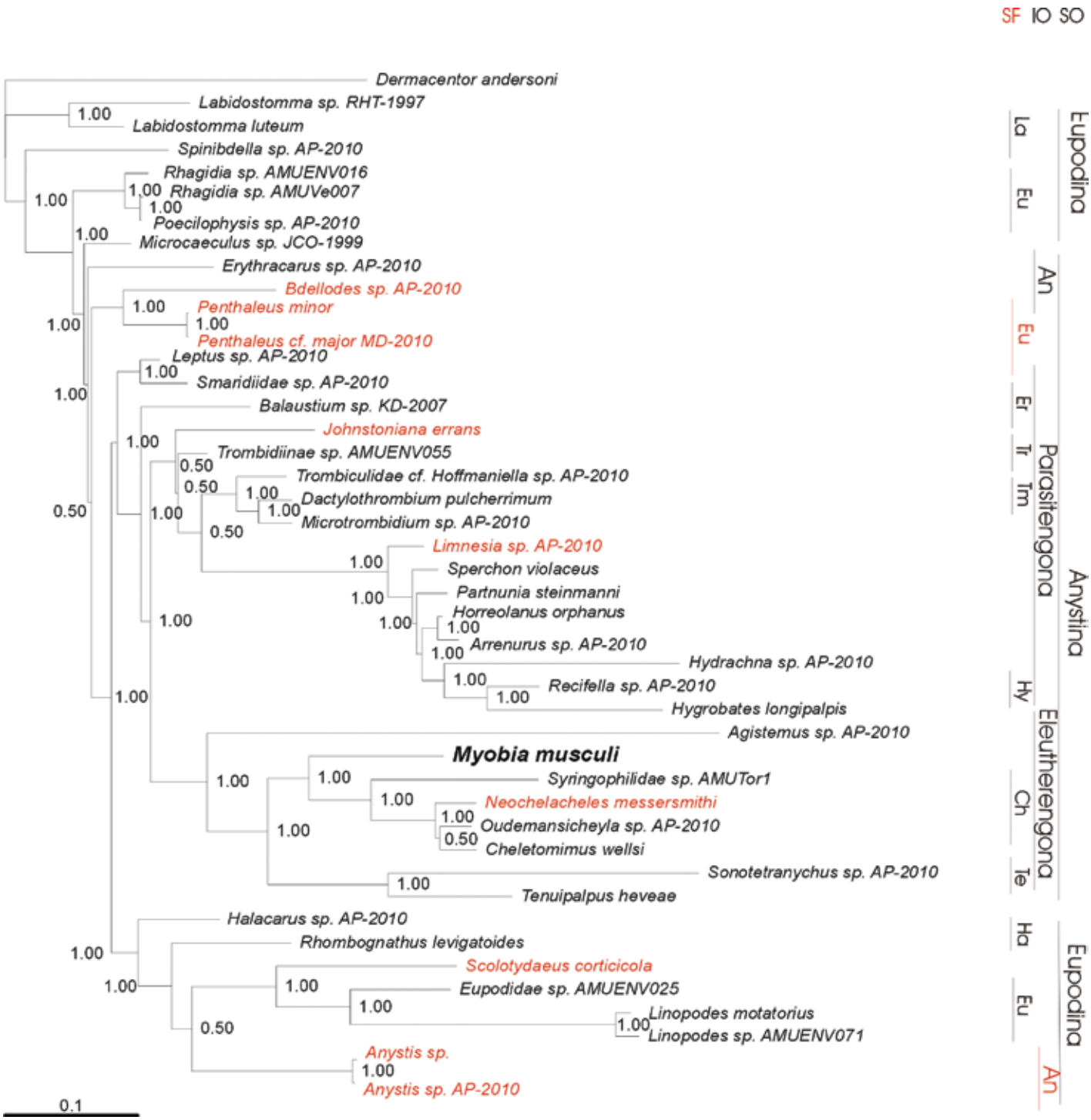

Figure 4. Depicted is the phylogram generated by Bayesian inference analysis of the *M. musculi* 18S rRNA sequence alignment showing the relationships among the Trombidiformes analyzed. Species highlighted in red are discrepant between historical and molecular taxonomic classification. SO, superorder; IO, intraorder; SF, superfamily; An, Anystae; La, Labidostommatoidea; Eu, Eupodoidea; Er, Erythraeoidea; Tr, Trombiculoidea; Tm, Trombidioidea; Hy, Hygrobatoidea; Ch, Cheyletoidea; Te, Tetranychoidea; Ha, Halacaroidea. The size bar represents the horizontal branch length associated with the expected nucleotide substitution probability per site.

that the secondary structure of the 5.8S rRNA region would be conserved because rRNA structure is critical to rRNA function. Thereafter, we performed a combination sequence and structural alignment using the RNAalifold server to resolve the location of this region in *M. musculi* and in addition identify the ITS1 and ITS2 regions. To our knowledge, lack of conservation of 5.8S rRNA nucleotide sequence between mite superfamilies has not been reported previously.

When reconstructing phylogenetic relationships among parasitiform mites, the 18S rRNA sequences are considered more appropriate for investigations at the level among phyla and superphyla, whereas the 28S rRNA sequence provides more signal at lower taxonomic levels.[18] Mites are very ancient: Trombidiformes arose 410 to 415 million years ago.[22] Mites are an example of extreme miniaturization of body plan, and the diverse taxons have remarkably different nucleotide substitution rates among lineages.[18] High nucleotide substitution rates are correlated with a short generation time and can lead to artifacts in molecular phylogenetic analyses.[16] Our analysis recapitulated previous results,[6] placing Labidostomatides as a cohort basal to the sister clades Anystina (Eleuthrengoinides and Parasitengonina) and the paraphyletic Eupodides, and terrestrial Parasitengonina as ancestral to Hydrachnidiae (water mites). In light of this previous analysis,[6] we restricted our sampling to the fast-evolving Trombidiformes and we retained ambiguous portions of the alignment to avoid artifacts due to long-branch effects. Our results, however, did not differ from those of the earlier study,[6] demonstrating that the phylogenetic relationships determined among Trombidiformes by using 18S rRNA sequence were not an artifact of the combination of sequences sampled. Our results also closely parallel those of a previous study (see Figure 5 B of reference 22), which combined molecular (18S rRNA) and morphologic data, although that study[22] showed basal relationships that were statistically not supported. Similarly, the relationships among the limited number of Trombidiformes analyzed by Bayesian inference of 18S rRNA and 28S rRNA in a previous study (see Figure 4 of reference 18) are identical to our study. Our analysis was limited by the lack of ribosomal gene sequence information available for other members of the subfamily Myobiinae. Given the diversity of Myobiinae parasitizing rodents and bats, research in this area is necessary if we are to understand the coevolution of these mammalian orders and Myobiinae.

References

1. **Altekars G, Dwarkakas S, Huelsenbeck JP, Ronquist F.** 2004. Metropolis-coupled Markov chain Monte Carlo for Bayesian phylogenetic inference. Bioinformatics **20:**407–415.
2. **Bernhart SH, Hofacker IL, Will S, Gruber AR, Stadler PF.** 2008. RNAalifold: improved consensus structure prediction for RNA alignments. BMC Bioinformatics **9:**474–487.
3. **Bochkov AV.** 1997. [New classification of myobiid mites (Acari, Acraiformes)]. Entomol Obozr **76:**938–951. [Article in Russian].
4. **Bochkov AV.** 2007. [Morphological adaptations of acariform mites (Acari: Acariformes) to permanent parasitism on mammals]. Parazitologiia **41:**428–458. [Article in Russian].
5. **Cannone JJ, Subramanian S, Schnare MN, Collett JR, D'Souza LM, Du Y, Feng B, Lin N, Madabusi LV, Muller KM, Pande N, Shang Z, Yu N, Gutell RR.** 2002. The Comparative RNA Web (CRW) site: an online database of comparative sequence and structure information for ribosomal, intron, and other RNAs. BMC Bioinformatics **3:**2.
6. **Dabert M, Witalinski W, Kzmierski A, Olszanowski Z, Dabert J.** 2010. Molecular phylogeny of acariform mites (Acari, Arachnida): strong conflict between phylogenetic signal and long-branch attraction artifacts. Mol Phylogenet Evol **56:**222–241.
7. **Evans GO, Sheals JG, Macfarlane D.** 1961. The terrestrial acari of the British isles, vol 1. Introduction and biology. London (UK): Trustees of the British Museum, Natural History.
8. **Ewing EF.** 1938. North American mites of the subfamily Myobiinae, new subfamily (Arachnida). Proc Entomol Soc Wash **40:**180–197.
9. **Fain A.** 1994. Adaptation, specificity, and host–parasite coevolution in mites (Acari). Int J Parasitol **24:**1273–1283.
10. **Fain A, Bochkov AV.** 2002. On some little known and a new species of Myobiidae (Acari) associated with rodents. Bulletin de la Societe Royale Belge d'Entomologie **138:**95–105.
11. **Felsenstein J.** 2004. PHYLIP (Phylogeny Inference Package) version 3.6. Distributed by the author. Seattle (WA): Department of Genome Sciences, University of Washington.
12. **Gambles RM.** 1952. *Myocoptes musculinus* (Koch) and *Myobia musculi* (Schranck), 2 species of mite commonly parasitizing laboratory mouse. Br Vet J **108:**194–203.
13. **Gruber AR, Lorenz R, Bernhart SH, Neuböck R, Hofacker IL.** 2008. The Vienna RNA websuite. Nucleic Acids Res **36:**W70–W74.
14. **Higgins DG, Bleasby AJ, Fuchs R.** 1992. CLUSTAL V: improved software for multiple sequence alignment. Comput Appl Biosci **8:**189–191.
15. **Hofacker IL.** 2003. Vienna RNA secondary structure server. Nucleic Acids Res **31:**3429–3431.
16. **Hofacker IL, Fekete M, Stadler PF.** 2002. Secondary structure prediction for aligned RNA sequences. J Mol Biol **319:**1059–1066.
17. **Institute for Laboratory Animal Research.** 1991. Infectious diseases of rats and mice. Common parasites: *Myobia musculi*, p 179–182. Washington (DC): National Academies Press.
18. **Klompen H, Lekveishivli M, Black WC 4th.** 2007. Phylogeny of parasitiform mites (Acari) based on rRNA. Mol Phylogenet Evol **43:**936–951.
19. **Livingston RS, Riley LK.** 2003. Diagnostic testing of mouse and rat colonies for infectious agents. Lab Anim (NY) **32:**44–51.
20. **Navajas M, Lagnel J, Fauvel G, De Moraes G.** 1999. Sequence variation of ribosomal internal transcribed spacers (ITS) in commercially important Phytoseiidae mites. Exp Appl Acarol **23:**851–859.
21. **Page RDM.** 1996. TREEVIEW: an application to display phylogenetic trees on personal computers. Comput Appl Biosci **12:**357–358.
22. **Pepato AR, Rocha CEF, Dunlop JA.** 2010. Phylogenetic position of the acariform mites: sensitivity to homology assessment under total evidence. BMC Evol Biol **10:**235–258.
23. **Posada D.** 2008. jModelTest: phylogenetic model averaging. Mol Biol Evol **25:**1253–1256.
24. **Pritchett-Corning KR, Csentino J, Clifford CB.** 2009. Contemporary prevalence of infectious agents in laboratory mice and rats. Lab Anim **43:**165–173.
25. **Reeves WK, Cobb KD.** 2005. Ectoparasites of house mice (*Mus musculus*) from pet stores in South Carolina, USA. Comparative Parasitology **72:**193–195.
26. **Tongson MS, Lasam OD.** 1982. A study of the prevalence of ectoparasites of house mouse (*Mus musculus*) in Diliman, Quezon City. Philippine J Vet Med **19:**15–21.
27. **Weisbroth SH, Friedman S, Powell M, Scher S.** 1974. The parasitic ecology of the rodent mite *Myobia musculi* I. Grooming practices. Lab Anim Sci **24:**510–516.